Talanta 308 (2026) 129812

Contents lists available at ScienceDirect

Talanta

journal homepage: www.elsevier.com/locate/talanta

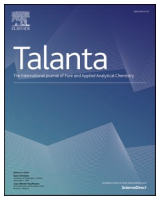

Improving ^{210}Po low level measurements in seawater

Á. López-Rodríguez [a,*], B. González-González [a], C. García-Prieto [a], J.L. Mas [b], F.A.C. Le Moigne [c], S.L.C. Giering [d], S. Hurtado-Bermúdez [a], M. Villa-Alfageme [a]

[a] Dpto. Física Aplicada II, ETSIE, Universidad de Sevilla, 41012, Sevilla, Spain
[b] Dpto. Física Aplicada I, ETSII, Universidad de Sevilla, 41012, Sevilla, Spain
[c] Laboratoire LEMAR. Institut Universitaire Européen de la Mer., 29280, Plouzané, France
[d] National Oceanography Centre, European Way, Southampton, SO14 3ZH, UK

ARTICLE INFO

Keywords:
^{210}Po
^{210}Pb
Radioactive disequilibrium
Co-precipitation
Ocean carbon storage
Biological carbon pump
Radiochemical speciation
α-spectrometry

ABSTRACT

The ocean is one of the largest sinks of atmospheric carbon. Surface phytoplankton absorb CO_2, forming the marine snow that sinks as a downward flux of particulate organic carbon (POC). A fraction of this POC flux reaches the deep ocean, where it can be stored for long periods of time. Quantifying this export flux enables us to estimate the ocean carbon sequestration. One of the most widely used methods of estimating the POC flux is measuring the disequilibrium of the radioactive pair ^{210}Pb-^{210}Po in the seawater column.

We present an accurate, robust method, easy-to-perform onboard during cruises, for measuring ^{210}Po and ^{210}Pb in seawater using $FeSO_4$ (Fe^{2+}) to co-precipitate polonium. This is a challenging step in seawater matrices, due to its high content in salt and organic matter, to which ^{210}Po is strongly bound. The method was validated with open-ocean samples collected on the PAP-Site Observatory. Replicate samples were processed employing a traditional method based on the co-precipitation with $Fe(OH)_3$ (Fe^{3+}). The co-precipitation method using $FeSO_4$ yields activities of ^{210}Po and ^{210}Pb that are consistent with previously reported values. In contrast, when co-precipitation is done using $Fe(OH)_3$ ^{210}Po is underestimated by an average of 40 ± 5% compared to co-precipitation with $FeSO_4$. Identical activity concentrations of ^{210}Po and ^{210}Pb, i.e. secular equilibrium, were expected in deep ocean waters, indicating the cease of the POC export. This was found using the $FeSO_4$ method, but a systematic deviation from the secular equilibrium was detected when precipitating with $Fe(OH)_3$, evidencing the ^{210}Po underestimation.

1. Introduction

The ocean is one of the largest active sinks for carbon dioxide, and the Biological Carbon Pump (BCP) is one of the main mechanisms by which CO_2 is removed from the atmosphere and exported to the deep ocean as particulate organic carbon (POC), over seasonal to decadal timescales. This POC is transported in the form of sinking particles that constitute marine snow, an heterogenous mix of particles mainly composed by plankton cells, fecal matter and biominerals [1]. Approximately 5 - 20 GTC yr^{-1} are globally exported from the surface to deep ocean by means of the BCP [2,3]. Any change in this mechanism could reduce the removal of atmospheric CO_2 by up to 50% [4,5]. Accurately quantifying the amount of POC exported and stored by the ocean through the BCP will help us to understand the evolution of atmospheric CO_2 in the next future.

A widely used approach to estimate downward POC fluxes is based on the distinct biogeochemical behavior of the naturally occurring radioisotopes from the ^{238}U series, ^{210}Po and ^{234}Th, relative to their respective parents, ^{210}Pb and ^{238}U respectively [6]. In this study, we focus on the ^{210}Pb – ^{210}Po pair, whose half-lives (128 days for ^{210}Po and 22.3 years for ^{210}Pb) [7] make it suitable for studying sinking POC fluxes on timescales of up to a few months [8].

In marine systems, ^{210}Pb is produced both from the in-situ decay of ^{226}Ra [9] and from the decay of atmospheric ^{222}Rn, through a series of short-lived products, to ^{210}Pb, which subsequently it is deposited onto the ocean surface [8,10]. The primary source of ^{210}Po in seawater is the in-situ decay of ^{210}Pb, being the ^{210}Po atmospheric deposition to the surface ocean almost negligible [11].

The concentration of both radioisotopes changes along depth, in the Euphotic Zone (EZ), where phytoplankton absorb atmospheric carbon [12] that sinks as POC flux, a ^{210}Pb – ^{210}Po disequilibrium arises from the preferential scavenging of ^{210}Po, relative to ^{210}Pb, by the sinking organic

* Corresponding author.
E-mail address: alopez49@us.es (Á. López-Rodríguez).

https://doi.org/10.1016/j.talanta.2026.129812
Received 26 January 2026; Received in revised form 7 April 2026; Accepted 9 April 2026
Available online 10 April 2026

matter [7]. In the upper Twilight Zone (TZ, >200 m), ^{210}Po excess is attributed to remineralization and fragmentation processes carried out by bacteria and zooplankton [13]. Deeper in the TZ, both ^{210}Po and ^{210}Pb are expected to reach secular equilibrium (i.e., equal activity concentrations), because no additional export and remineralization processes take place [6]. Determining the disequilibrium of both radioisotopes in depth allows to estimate the ^{210}Po downward flux, which is used as a proxy to calculate POC flux [7].

^{210}Po is commonly determined by alpha spectrometry, which provides very low detection limits [14]. Before the radiochemical preparation ^{210}Po must be extracted, isolated and concentrated from the sampled matrix. In seawater, ^{210}Po extraction is particularly challenging because of the complexity of this matrix, which contains high salt concentration and organic matter to which ^{210}Po is strongly bound [14,15].

In most of the oceanographic cruises this extraction method must be performed on board to minimize the amount of water stored and transported to the laboratory. Therefore, ^{210}Po measurement methods in oceanography must benefit from being robust, straightforward, and quick to implement on board.

A traditional approach for ^{210}Po extraction relies on its co-precipitation using a precipitating agent. The most common agent is $Fe(OH)_3$ (Fe^{3+}) [16,17], however, cobalt–ammonium pyrrolidine dithiocarbamate (Co-APDC) has been gaining popularity in the recent years [18]. A polonium isotope, usually ^{209}Po is usually added as spike [19,20].

For the method based on polonium co-precipitation using Fe^{3+}, there is extensive literature reporting analytical problems in the measurement of ^{210}Po and its disequilibrium in depth with ^{210}Pb in seawater matrices. Results from previous intercalibration studies [21–23] and several oceanographic cruises [6,24–27] pointed out that ^{210}Po and ^{210}Pb do not consistently reach the expected secular equilibrium in deep waters when the Fe^{3+} method is used. This lack of expected secular equilibrium with its parent ^{210}Pb in deep waters can be explained by the fact that this method underestimates ^{210}Po activity in the samples [27,28].

This is an important issue for downward POC flux evaluations, as the analytical inaccuracies in ^{210}Po and ^{210}Pb activity determination are directly propagated to the accuracy of the POC fluxes derived from this method [23].

Hence, in recent years, there has been a growing interest in developing alternative, reliable methodologies to accurately, precisely and routinely measure ^{210}Po and ^{210}Pb in seawater samples [25,29–32]. While the Co-APDC approach has proven to provide robust results in the determination of ^{210}Po and ^{210}Pb in seawater [27], it is a laborious and time-consuming method to apply on board during oceanographic cruises.

In this context, the method based on the co-precipitation of ^{210}Po and ^{209}Po with $FeSO_4$ (Fe^{2+}) has been employed for the determination of other actinides in seawater, such as ^{236}U and ^{237}Np [33–35]. Moreover [31], successfully applied it for the determination of ^{210}Po in freshwater matrices.

In this study, we apply this approach to the determination of ^{210}Po and ^{210}Pb in seawater matrices. Our method was first implemented to determine ^{210}Po activities in groundwater samples and ^{210}Po in coastal surface seawater. Thereafter, the method was extended to obtain high-resolution ^{210}Po–^{210}Pb depth profiles in open-ocean seawater samples collected during two oceanographic campaigns around the PAP-Site Observatory in the North Atlantic. For comparing and validating the performance of the results, several replicates were collected and processed using the traditional Fe^{3+} method and deep ocean samples were measured using both methods, in order to test secular equilibrium in the absence of particulate export.

2. Sampling and methods

2.1. Sampling

To set up and validate the method, a total of 94 samples from different unfiltered water matrices — including freshwater from wells, coastal surface and open-ocean samples — were collected and ^{210}Po, and sometimes ^{210}Pb, were determined.

Furthermore, to demonstrate the robustness of the Fe^{2+} method, different elapsed times between sampling, processing, and measurement were tested, including immediate ^{210}Po determination, one-year storage, and a dual approach for ^{210}Po and ^{210}Pb determination. This comprehensive analysis across various water matrices and different elapsed times was carried out to validate the metho to overcome the lack of available, accurately evaluated, reference water matrices for ^{210}Po [36].

All samples were immediately acidified to pH 3 after collection to prevent the adsorption of metals or radionuclides to container walls, minimize microbial degradation, and keep species in solution, 10 mL of nitric acid were used per 5 L of water, and stored dark until further processing. Each sample was also spiked with 0.2 Bq of ^{209}Po to assess polonium recovery during the radiochemical procedure and gently shaken for 2 min. When samples were processed in the laboratory and not on the ship, to simulate the procedure followed on board, only six to 8 h were allowed for homogenization to take place.

2.1.1. Freshwater

Groundwater samples were collected in the influence area of the Uranium Factory of Andújar (FUA), in Jaén, which is currently under decommissioning. Specifically, three locations were sampled (Fig. S1, Supplementary Material). Samples were collected during the environmental radiological monitoring program of the Consejo de Seguridad Nuclear (CSN) in January 2021. Groundwater samples were stored for one year after collection before ^{210}Po determination.

The unfiltered water volumes collected in the three sampling points were split into 1 L aliquots and grouped into batches denoted as A, B, and C (Table 1). Half of the aliquots from each batch were processed using the Fe^{2+} method, and the other half were replicates processed using the Fe^{3+} method for intercalibration.

2.1.2. Coastal surface seawater

Coastal surface seawater samples were collected at two locations in the Gulf of Cádiz, Spain: Huelva (December 2021) and Cádiz (March 2022). Sampling coordinates are shown in Fig. S1.

These unfiltered samples were split into 5 L aliquots and grouped in different batches. The total sample volume collected in Huelva was split into 4 aliquots (Batch D, Table 1), and the sample volume from Cádiz into 18 aliquots, grouped into Batches E to H. Half of the aliquots from each batch were processed using the Fe^{2+} method, while the replicates were processed using the Fe^{3+} method for intercalibration.

2.1.3. Open-ocean seawater profiles

To test the Fe^{2+} method in open ocean seawater, a total of 87 samples from 0 to 600 m depth with a CTD-rosette and Niskin bottles were collected in two different oceanographic cruises at the Porcupine Abyssal Plain Observatory (PAP-Site, 48° 50′ N 16° 30′ W, 4850 m depth) to obtain high resolution ^{210}Po - ^{210}Pb depth profiles. This multidisciplinary observatory is an open-ocean, long-term time series site in the NE Atlantic, focusing on the study of the connections between the surface and the deep ocean [37].

A first unfiltered water profile was collected during the *JC231* cruise, on 18 May 2022, on board the *RRS James Cook* led by the National Oceanography Centre (NOC). The goal of the cruise was to continue time-series observations on the surface ocean, water column, and seafloor at the site. The station sampled during this campaign was labelled SS1-1 (Table S1, Fig. 1).

Table 1
Total ^{210}Po activity concentrations (Bq·m^{-3}) and chemical yields (R%) obtained with the Fe^{3+} and Fe^{2+} methods in duplicate samples and batch averages from groundwater (Jaén) and surface seawater (Cádiz and Huelva). Uncertainties are reported as absolute values (±σ) and percentages (%).

Study Area	Batch	Samples duplicates								Batches average							
		Fe^{3+}				Fe^{2+}				Fe^{3+}				Fe^{2+}			
		^{210}Po	± σ	%	R%	^{210}Po	± σ	%	R%	^{210}Po	± σ	%	R%	^{210}Po	± σ	%	R%
Uranium mine	A	6.7	1.8	27	36	7.7	1.9	25	60	7.4	1.7	23	48 ± 8	7.8	2.0	26	61 ± 8
Jaén, Spain		5.7	1.5	26	53	6.3	1.4	26	50								
38.21 °N, 4.1 °W		7.3	1.9	26	48	6.6	1.3	23	65								
17/01/2021		9.7	1.6	16	55	10.6	0.5	5	68								
	B	2.4	0.4	29	60	4.2	0.8	19	51	2.6	0.1	21	64 ± 4	3.8	0.6	18	53 ± 3
		2.7	0.7	26	66	4.1	1.0	24	56								
		2.7	0.3	11	67	3.0	0.2	7	51								
	C	4.9	0.5	10	45	4.7	0.3	6	55	4.9	0.5	10	45 ± 0	4.7	0.3	6	55 ± 0
		22	4	18	49	18	2	11	54								
Punta Umbría	D	2.7	0.5	19	55	3.0	0.4	13	55	2.3	0.6	26	64 ± 13	3.0	0.1	3	50 ± 8
Huelva, Spain		1.8	0.2	11	73	2.9	0.5	17	44								
37.2 °N, 7.0 °W																	
8/12/2021																	
Playa de la	E	3.0	0.8	30	49	3.5	0.7	20	43	2.7	0.5	19	49 ± 0	3.7	0.3	8	50 ± 9
Cortadura		2.3	0.4	17	49	3.9	0.4	10	56								
Cádiz, Spain	F	6.7	1.1	16	55	6.9	0.8	12	55	4.9	1.8	37	55 ± 3	5.2	1.6	31	52 ± 8
36.5 °N, 6.3 °W		4.9	1.0	20	50	3.8	0.5	13	59								
18/03/2022		3.2	0.6	19	55	4.8	0.8	17	43								
	G	6.7	1.1	16	55	14	2	14	53	10.7	2.5	23	60 ± 4	13	2	15	50 ± 3
		11	2	18	58	15	2	13	50								
		11	2	18	65	11	2	18	48								

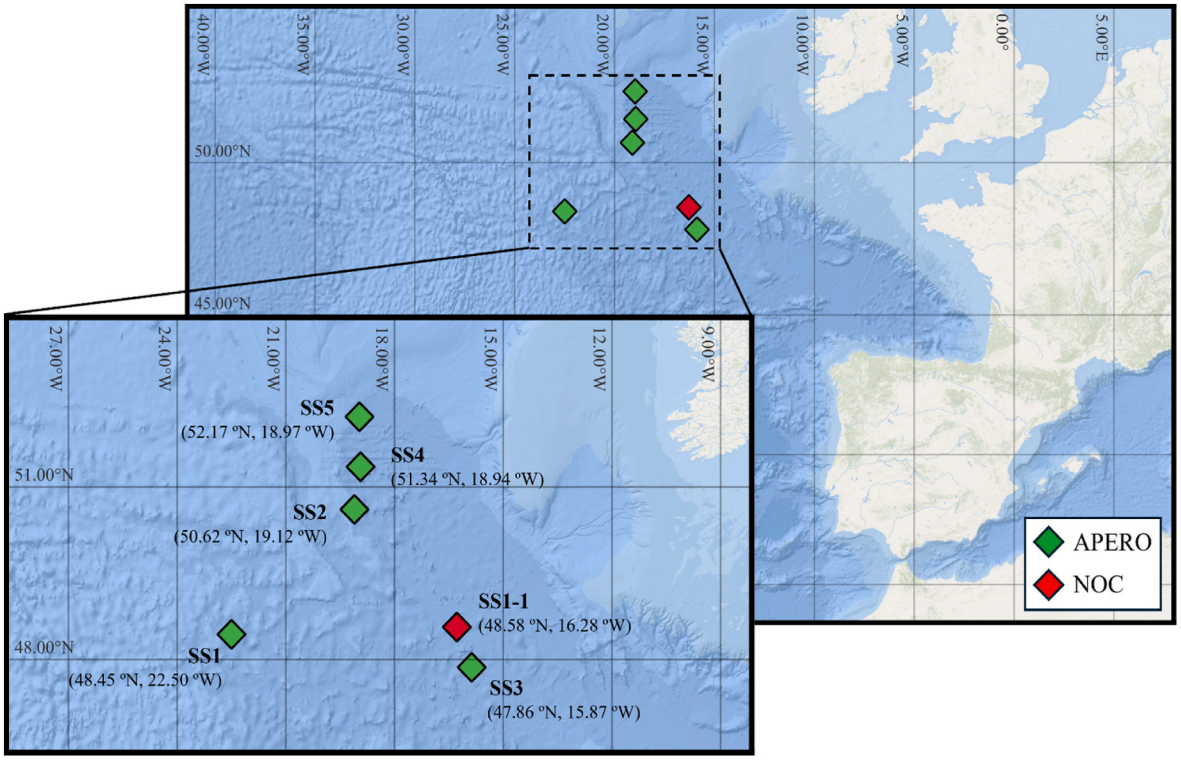

Fig. 1. Stations sampled during the NOC (Red) and APERO (Green) campaigns around the PAP-SO in spring 2022 and summer 2023, respectively.

Five additional profiles were sampled the following year, between 6 June and 17 July 2023, on board *Pour Quoi Pas?* during APERO cruises. APERO project aims to study the mechanistic functioning of the BCP with emphasis on the mesopelagic ocean [38]. Stations sampled during this campaign were labelled from SS1 to SS5 (Table S1, Fig. 1).

Replicates were collected at several depths in both cruises and processed using the Fe^{3+} co-precipitation method (Table S1).

2.2. $Fe(OH)_2$ co-precipitation method

Below we describe the steps followed for ^{210}Po determination in 5 L water samples.

Step 1. *Preconcentration of lead and polonium*

The radiochemical procedure starts by adding 1.25 g of $FeSO_4$ (Fe^{2+}) and 2.5 g of $K_2S_2O_5$ to the spiked samples. $K_2S_2O_5$ prevents Fe^{2+} from

oxidizing. The samples are gently shaken for 2 min, after which the pH is adjusted to 8 – 9 using 20 mL of concentrated NH_4OH (13 M), resulting in the formation of $Fe(OH)_2$ precipitate. The precipitate is allowed to settle for at least 24 h, after which it is siphoned off, and the precipitate – carrying the dissolved fractions of ^{210}Pb, ^{210}Po, and ^{209}Po – is transferred to 250 mL bottles.

Step 2. *Sample conditioning*

The precipitate from each sample is evaporated to near dryness at a controlled temperature of 60 °C to avoid polonium losses due to volatility [39]. The precipitate is then dissolved using 10 mL of 37% HCl and 1 mL of H_2O_2. This evaporate–dissolve procedure is repeated three times to ensure complete digestion of the organic matter and to bring the solution to an acidic medium. The final residue is dissolved in 120 mL HCl (1 M).

Step 3. *Separation of polonium from lead*

The polonium isotopes ^{210}Po and ^{209}Po were spontaneously deposited onto silver discs (25 mm diameter). To this end, 0.2 g of ascorbic acid was first added to prevent any iron in the sample from interfering with polonium plating. A one-side coated silver disc was then introduced, suspended from a nylon thread, and the bottles were tightly capped and heated at 60–70 °C for at least 8 h. A deposition time of more than 4 h is recommended for optimal recoveries [40]. Finally, the silver discs were retrieved, rinsed with distilled water, and allowed to dry.

Is important to note that to avoid an statistical increase of the uncertainties of the ^{210}Po and ^{210}Pb activity concentrations, the elapsed time between the collection of the sample at open sea and the final separation of ^{210}Po by its deposition onto silver disks must be minimized [41], due the relatively short ^{210}Po half-life ($T_{1/2} = 138$ days).

An intercomparison of methods was performed using the co-precipitation of polonium and lead through the previously employed Fe^{3+}. In that co-precipitation method steps 2 and 3 remained the same, while Step 1 substitute $FeSO_4$ for $FeCl_3$ as carrier to form Fe^{3+} instead. Specifically, 10 mL (0.250 g/mL) of $FeCl_3$ were added. $Fe(OH)_3$ and polonium were co-precipitated after adjusting the pH to 8–9 with 20 mL of NH_4OH [42].

2.3. Instrumentation and α – measurement

^{209}Po and ^{210}Po activities were determined at CITIUS (Centro de Investigación, Tecnología e innovación, Universidad de Sevilla) laboratory at the Universidad de Sevilla by alpha spectrometry using PIPS detectors with 450 mm^2 active area and 18 keV resolution at the highest alpha emission energy of ^{241}Am (5.486 MeV) for at least one week to guarantee that uncertainties were lower than 5%. The alpha background count rates (cps) contributed on average less than 1% to the total counts of ^{210}Po and ^{209}Po (10^{-6} cps for ^{210}Po and 10^{-5} cps for ^{209}Po). To obtain ^{210}Po at the sampling date in the different water matrices, decay corrections were applied based on the time elapsed between sample collection and measurement, additional corrections had to be performed when ^{210}Pb activities were measured [40].

Specifically, coastal surface seawater samples from Huelva and Cádiz (Spain) were processed and measured immediately after collection for ^{210}Po determination, yielding activities approximately corresponding to the sampling date. For groundwater samples collected in Jaén (Spain) and stored for one year, ^{210}Po activity at the sampling date cannot be obtained any longer, as after a year it is in secular equilibrium with its parent ^{210}Pb. In that case ^{210}Pb and ^{210}Po, both in secular equilibrium, at the sampling date are provided indirectly through the measurement of ^{210}Po. Finally, open-ocean samples collected during the PAP cruises were processed using the double-measurement approach detailed in studies such as [40] to obtain both ^{210}Po and ^{210}Pb at the sampling date. More details about the measurement procedure and decay corrections of ^{210}Po and ^{210}Pb in the different water matrices are provided in Section S1 of the Supp. Material.

3. Results and discussion

3.1. Measurement of the activity concentration

3.1.1. Groundwater and coastal surface seawater

Table 1 presents ^{210}Po activity concentrations and the average of each batch for groundwater and coastal surface seawater samples following our Fe^{2+} co-precipitation method described in Section 2.

Groundwater was collected from an area influenced by the FUA (Fig. S1); in areas where uranium is mined and extracted, ^{210}Po and ^{210}Pb tend to accumulate in tailings and run-off [43]. Determined ^{210}Po activities were similar between aliquots, with the average batch standard deviation of ^{210}Po narrowly ranging from 6 to 26%. Moreover, these values are in close agreement with the uncertainties associated with individual aliquots, which ranged from 5 to 26%. The only exception was Batch C, where one duplicate showed markedly higher activity than the other replicates (18 ± 2 Bq·m^{-3}). As indicated below, this duplicate also exhibited the highest ^{210}Po activity measured using the Fe^{3+} method (22 ± 4 Bq·m^{-3}). Nevertheless, since the samples were collected at three different sampling points, variations between aliquot batches are expected.

These values fall within the range reported for Spanish groundwater (1.4 – 78 Bq·m^{-3}, average 20 ± 7 Bq·m^{-3} [44]) and for slightly contaminated groundwater in the uranium-mineralized area of Jaduguda, India (average 9.3 ± 2.1 Bq·m^{-3} [43]). Other regions affected by uranium mining exhibit much higher ^{210}Pb levels [45].

For coastal surface seawater, average ^{210}Po standard deviations also align with individual aliquot uncertainties in all batches. Seawater samples from Cádiz were measured in consecutive weeks, so a small fraction of ^{210}Po originated from ^{210}Pb ingrowth during the elapsed time. This explains the slight increase in ^{210}Po activity observed from batches E to G, despite identical sampling time and matrix. By contrast, replicates within the same batch were analyzed on the same day, and the results were within the uncertainty.

^{210}Po activities determined in surface seawater samples show good agreement among those collected in Huelva and Cádiz (Batches D to G). These values also fall within the range reported in the literature for coastal surface waters (0.25 – 3.39 Bq · m^{-3} [46–51]) and specifically align with previously reported ranges values for the southern Atlantic coast (0.50 – 1.94 Bq·m^{-3} [48,52]).

3.1.2. ^{210}Po – ^{210}Pb depth profiles from PAP-site campaigns

Fig. 2 plots ^{210}Pb – ^{210}Pb depth profiles obtained from both NOC (SS1-1) and APERO (SS1 to SS5) campaigns using Fe^{2+}. ^{210}Po and ^{210}Pb activity concentrations and their ratio ($^{210}Po/^{210}Pb$) are shown in Table S1. Determined values for both radioisotopes during the two cruises align well with those reported in previous PAP-site studies, ranging from 0.45 to 2.1 Bq·m^{-3} for ^{210}Po and from 1.06 to 6.7 Bq·m^{-3} for ^{210}Pb [7,53,54].

To correctly interpret depth profiles from Fig. 2 we differentiate two regions in the water column. The euphotic zone (EZ), from 0 to 126.5 m in the sampled stations, is the layer that receives enough solar radiation to allow phytoplankton photosynthesis and therefore the production of organic matter [55]. The euphotic zone base (EZB in Fig. 2) is taken as the depth of 0.1% light penetration [6]. In the twilight zone (TZ), below the EZB, there is no further production of organic matter [56].

In the EZ, all stations exhibit ^{210}Po deficits relative to ^{210}Pb ($^{210}Po/^{210}Pb$ ratios average 0.71 ± 0.05), due to preferential ^{210}Po scavenging [13]. Indeed, whereas ^{210}Pb is only adsorbed on particles surface, ^{210}Po is strongly adsorbed on particles, but also incorporated to phytoplankton cells, and bioaccumulated through the food web [57–59].

In the TZ, $^{210}Po/^{210}Pb$ ratios are closer to 1 (average 0.97 ± 0.07)

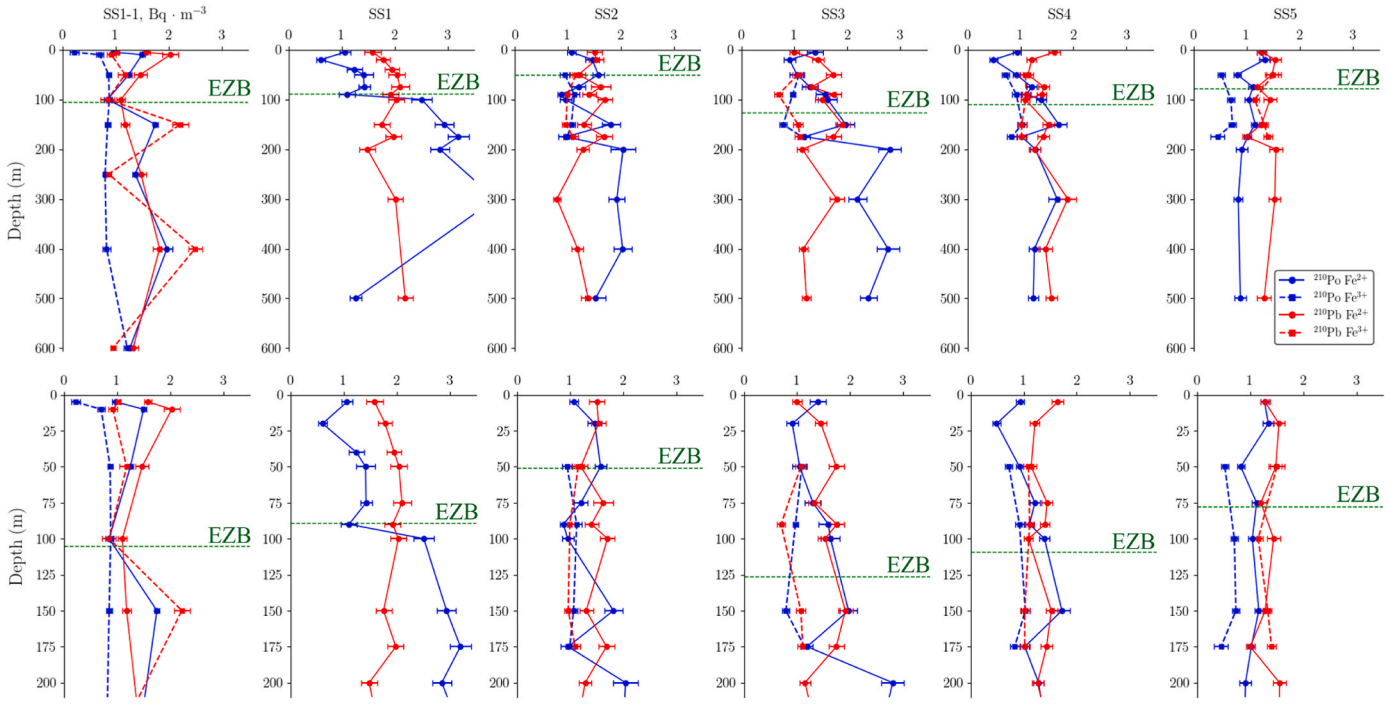

Fig. 2. (Top) ^{210}Po (Blue filled circle) and ^{210}Pb (Red filled diamond) activity concentration (Bq · m^{-3}) depth profiles measured with Fe^{2+} (straight line) and Fe^{3+} (dashed line) methods. (Bottom) 200 m - zoom.

due to the absence of net removal or ^{210}Po addition occurring faster than their ingrowth–decay [17]. Profiles SS1, SS2 and SS3 show ^{210}Po excess values in relation to ^{210}Pb (^{210}Po/^{210}Pb > 1) from 250 m downward that likely reflects the release of particulate ^{210}Po to non-sinking phases through remineralization or disaggregation processes carried out by bacteria and zooplankton [13].

Our results align well with those reported by Ref. [60], who presented ^{210}Po – ^{210}Pb depth profiles along a North Atlantic transect during the GEOVIDE program. In this cruise the Co-APDC method was obtained for polonium co-precipitation. Two of their sampled stations were located near the PAP Site (Stations 21 and 26; see Fig. 1 in the article). Fig. S2 shows average ^{210}Po – ^{210}Pb activities obtained during the NOC and APERO campaigns and those from GEOVIDE. In addition to the good agreement observed in the range of measured values for ^{210}Po and ^{210}Pb, both radioisotopes show similar vertical patterns in the water column: ^{210}Po deficits in the EZ (~50 m) due to particle scavenging, and either secular equilibrium or ^{210}Po excesses below ~ 250 m in the TZ.

As a final remark of the excellent performance of the method here presented, during the APERO campaign, POC and ^{210}Po fluxes were determined from the ^{210}Po – ^{210}Pb disequilibrium, using the Fe^{2+} method, and complementary using sediment traps. The results show an excellent agreement at the ten depths in the five stations where the fluxes were evaluated using both methods [61].

3.2. *Evaluation of the performance of the Fe^{2+} co-precipitation*

3.2.1. *Chemical yields*

Table 1 shows the individual and batch-averaged chemical yields for groundwater and coastal surface seawater samples. Table S1 includes the chemical yields obtained for the collected open ocean samples from PAP cruises. Additionally, Fig. S3 presents the boxplot summarizing the chemical yields statistics obtained for all analyzed matrices.

The higher chemical yields observed in groundwater matrices compared with coastal surface seawater, and especially with open-ocean samples, both in terms of average and quartile values, have already been reported previously, 40 – 87% for groundwater samples [60,62–64] and from 20 to 71% in seawater [7,12,13,39,65,66]. As further discussed below, there are at least two factors that complicate ^{210}Po extraction from seawater matrices: the high salinity [42], and the high content of organic matter [27,67,68].

The overall lower chemical yields measured when applying Fe^{2+} method relative to Fe^{3+} (Table 1 and boxplot in Fig. S3) is likely related to the formation of smaller aggregates in the Fe^{2+} than in the Fe^{3+} precipitates, which takes longer times to completely settle than the processing time on board, and are therefore partially lost during the siphoning process. Nevertheless, these losses are accounted for in the measurement process and ^{210}Po activity is still accurately determined.

3.2.2. *Intercomparison of Fe^{2+} and Fe^{3+} co-precipitation methods*

^{210}Po activity underestimation.

Fig. 3 plots ^{210}Po activity concentrations determined in all replicate samples processed using the Fe^{3+} (x-axis) and Fe^{2+} (y-axis) co-precipitation methods. These results include groundwater and coastal seawater samples (Fig. S1) and the open-ocean water samples collected during the two campaigns conducted around the PAP site (Fig. 1). The complete dataset results can be found in Table 1 and S1, respectively. Additionally, Figs. S4 and S5 include boxplots summarizing the statistics results obtained for replicates processed using co-precipitation with Fe^{2+} and Fe^{3+}.

The smallest differences between the two methods were observed in the groundwater samples, where the results cluster close to the 1:1 line (Fig. 3). Within uncertainties, individual aliquots yielded the same activity in eight of the nine replicates and the average ^{210}Po activities and quartile values were consistent within methods (Fig. S4).

Differences were more pronounced in coastal surface and open-ocean samples. Indeed, most of the results for these matrices lie above the 1:1 line in Fig. 3. In coastal samples, although average ^{210}Po values overlap within uncertainties, the boxplot (Fig. S4) clearly shows a systematic shift toward higher activities for Fe^{2+} co-precipitation in relation to Fe^{3+}. This is evidenced by consistently larger quartile values (Q_1, median, and Q_3), indicating that the difference is not driven by a few high values but reflects an overall higher activity across the entire dataset.

The most notable differences were observed in the open-ocean

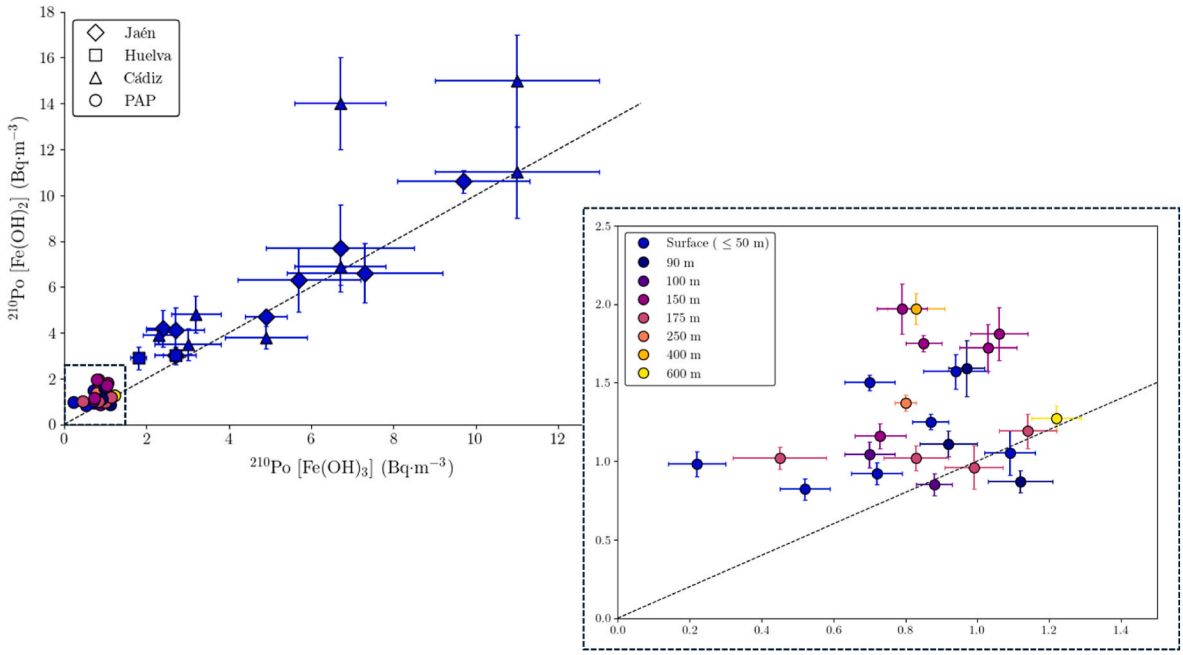

Fig. 3. ^{210}Po activity concentrations (Bq · m^{-3}) determined using the Fe^{3+} (x-axis) and Fe^{2+} (y-axis) methods. The 1:1 line ($y = x$, black dashed line) is also plotted. The zoomed figure (lower right) shows the results for open-ocean samples differentiated by depth.

samples from PAP cruises (Fig. S5). In the EZ, average ^{210}Po activity with the Fe^{2+} method was 38 ± 11% higher relative to the Fe^{3+} method. In the TZ, these differences were even more pronounced, with average ^{210}Po activities 53 ± 12% higher. In both cases, the shift was not limited to mean values: all determined quartiles were consistently higher with the Fe^{2+} method, similarly to coastal waters.

The underestimation when the co-precipitation is performed using Fe^{3+} takes place in 23 out of 42 replicates across all water matrices analyzed in this study. In 18 replicates both methods yield the same activity (mostly groundwater), and only in one replicate does the Fe^{2+} method underestimate ^{210}Po activity. In coastal and open-ocean water samples, the Fe^{3+} method underestimates ^{210}Po activity by an average of 46 ± 8% [21]. also reported an underestimation of 35% for the comparison between replicates processed with Fe^{3+} and Co-APDC methods.

The systematic higher concentrations found when performing co-precipitation with Fe^{2+} from the open-ocean samples is depth-independent within each region, as shown in the zoomed view of Fig. 3. Although the underestimation is higher in the TZ relative to the EZ, there is no relationship with depth in either region. This consistency indicates that the observed underestimation is not due to replicate bias or depth-dependent biological or biogeochemical processes within the water column but rather reflects a methodological bias inherent to the Fe^{3+} approach.

^{210}Po – ^{210}Pb secular equilibrium in the water column.

Fig. 2 also includes in dashed lines the ^{210}Pb – ^{210}Pb depth profiles obtained by applying the Fe^{3+} method in the replicates collected from both NOC and APERO cruises (See data in Table S1). This Figure graphically shows that within uncertainties, the Fe^{3+} method clearly underestimates ^{210}Po activity in most of the samples, as previously discussed.

^{210}Po deficits in the EZ are due to its preferential scavenging relative to ^{210}Pb onto sinking organic matter [13]. Although these deficits are observed using both methods, ^{210}Po underestimation with the Fe^{3+} method led to ^{210}Po/^{210}Pb ratios in the EZ that were underestimated by 15 – 47% (averaging 19 ± 11 %) relative to Fe^{2+} (Fig. S3).

This bias becomes even more evident in the TZ. In this region export events no longer take place and both radioisotopes are expected to reach secular equilibrium [6]. Using the Fe^{2+} method ^{210}Po and ^{210}Pb indeed reach a consistent equilibrium, with ^{210}Po/^{210}Pb ratios averaging 0.97 ± 0.07 ($Q_2 = 1.0$ and $Q_3 = 1.1$ in Fig. S5). In contrast, the Fe^{3+} method yielded a pronounced disequilibrium, ^{210}Po/^{210}Pb ratios obtained with the Fe^{3+} method were on average 32 ± 9% lower than those obtained with Fe^{2+}, with 75% of the results falling below secular equilibrium ($Q_3 = 1.0$ in Fig. S5) and average ratios of 0.79 ± 0.08. As a result, the Fe^{3+} approach biases the ^{210}Pb – ^{210}Po disequilibrium at depths where the Fe^{2+} method indicates that secular equilibrium has already been established.

In detail, at station SS1-1 both radioisotopes consistently reach secular equilibrium throughout the TZ when using the Fe^{2+} method, whereas this equilibrium is disrupted by large ^{210}Po deficits within the TZ at 150 and 400 m when using Fe^{3+}. A similar pattern is observed at most stations sampled during APERO cruises: at stations SS3 and SS5, secular equilibrium along the TZ is observed only with the Fe^{2+} method and is not achieved with Fe^{3+} due to ^{210}Po deficits. Station SS4 is the only where the two methods yielded a consistent and similar secular equilibrium.

Furthermore, ^{210}Po excess values (^{210}Po/^{210}Pb > 1) determined in the TZ during APERO are consistent with the depths of bacterial and zooplankton remineralization and fragmentation processes reported in Ref. [38]. However, ^{210}Po/^{210}Pb ratios obtained with the Fe^{3+} method, showing underestimation, can lead to a misinterpretation of these processes. For example, at 150 m in SS2, the intensive POC fragmentation reported in Ref. [38] would be consistent with the ^{210}Po peak determined with the Fe^{2+} method. In contrast, the Fe^{3+} method indicated secular equilibrium between the two radioisotopes, and based on this, the fragmentation process would not be identifiable.

Thus, ^{210}Po and ^{210}Pb underestimation when Fe^{2+} is employed for polonium co-precipitation leads to a more consistent secular equilibrium below the export zone between the two radioisotopes, while it is disrupted in the TZ with Fe^{3+}. In the literature, ^{210}Po deficits, and thus ^{210}Po - ^{210}Pb disequilibrium in deep waters, are typically explained from the unequal adsorption and desorption processes affecting sinking particulate matter [69], or to ^{210}Po being scavenged in unorthodox ways by deepen phytoplankton [21,23,46,70]. In this study, we find that such deep ^{210}Po deficits occur more frequently when the Fe^{3+} method is employed compared to Fe^{2+}. Similarly [21], reported more consistent

equilibrium between both radioisotopes when using the Co-APDC method relative to the Fe^{3+} method.

3.3. Unravelling the uncomplete extraction of polonium in seawater

3.3.1. Functioning of the different methods for polonium and lead co-precipitation

The Fe^{3+} co-precipitation method was already applied in the 60s [71], and is currently the most widely used technique for determining ^{210}Po in seawater [27,72]. However, there is extensive literature reporting analytical problems in the measurement of ^{210}Po and its disequilibrium in depth with ^{210}Pb with this method [27].

Three groups were first to report problems in the measurement of ^{210}Po and ^{210}Pb in seawater samples during the GEOSECS program [21–23]. Specifically [21], reported ^{210}Po deficiencies relative to ^{210}Pb in the TZ, which were not observed when applying the Co-APDC method.

Unexpected ^{210}Po deficits observed in even deeper waters (up to 3000 m) were also reported in the intercalibration exercise conducted during the GEOTRACES program [23], as well as in numerous other campaigns which applied the Fe^{3+} method [6,24–27]. The recent study [27] reported that, among the 213 depth profiles analyzed, ^{210}Po – ^{210}Pb disequilibrium at depths >300 m occurred in twice as many profiles when using the Fe^{3+} method compared with Co-APDC. In addition, they found that the Fe^{3+} method systematically underestimated ^{210}Po activity concentrations by an average of 35%. Both findings were also reported in Ref. [73]; a more consistent secular equilibrium was observed with the Co-APDC method relative to $Fe(OH)_3$, and a^{210}Po underestimation with Fe^{3+} ranging between 8 and 24%.

Interestingly, underestimated activities are not limited to ^{210}Po [22]. also reported a systematic underestimation of ^{210}Pb using the Fe^{3+} method of 30% relative to Co-APDC. However [27,73], found statistically similar ^{210}Pb activities between the two methods (Fe^{3+} and Co-APDC).

The Co-APDC method has proven highly effective and robust for isolating ^{210}Po from seawater in numerous oceanographic campaigns [27,52,74–78]. As the only disadvantage, it requires the individual filtration of every sample after co-precipitation of polonium with the insoluble Co-APDC chelate [18], making the method labour-intensive and time-consuming on board.

By contrast, the Fe^{2+} method enables the precipitate to be easily recovered by siphoning, making it ideal for oceanographic cruises. Its simplicity and efficiency are particularly valuable when processing large seawater volumes at multiple stations.

3.3.2. ^{210}Po speciation in seawater

There are different reasons that account for the observed ^{210}Po deficits measured using the Fe^{3+} method. ^{210}Po activity is determined from the count-rate ratio of ^{210}Po to ^{209}Po, multiplied by the known activity of ^{209}Po [27,40] (Equation S(1) in Supp. Material). This equation assumes that ^{210}Po and ^{209}Po are chemically equivalent, and recovered in the same proportion (i.e., with the same chemical yield) during the polonium isolation step (Section 2). However, as it is suggested by Ref. [23], obtaining the same extraction of ^{210}Po and ^{209}Po strongly depends on the co-precipitation method applied.

The unequal extraction of ^{210}Po and ^{209}Po explains the underestimation of ^{210}Po activity observed with the Fe^{3+} method in the analyzed replicates.

The divergences could arise due ^{209}Po not being efficiently recovered during the radiochemical method, under or overestimating the amount ^{209}Po in the sample. In the case of a^{209}Po underestimation, the ^{210}Po results would be overestimated, therefore, the hypothesis of an incomplete recovery of the spike ^{209}Po is ruled out, as the results clearly show an underestimation of ^{210}Po. A^{209}Po overestimation, originated by a systematic contamination during the radiochemical separation, would produce lower ^{210}Po, however, the blanks prepared for the different batches do not show any additional contribution of ^{209}Po, and more importantly, the underestimation of ^{210}Po results is found systematically across cruises.

Therefore, the underestimation of ^{210}Po with Fe^{3+} must be due, conversely, to a deficient extraction of ^{210}Po relative to ^{209}Po. This hypothesis considers that the spike ^{209}Po is correctly co-precipitated, but ^{210}Po is not recovered in the same proportion. This explanation was first proposed by Ref. [23] and later supported by the results of several studies [27,28,79].

The time available on the ship between the sample pre-conditioning and the co-precipitation method is about 8 h. During this time, the speciation of both radioisotopes, ^{210}Po and ^{209}Po, may not be homogeneous. While ^{209}Po is added in mineral phase (i.e in acidic solution) a few hours before the co-precipitation, ^{210}Po is strongly bound to organic matter [15], dissolved organic matter (DOM) ligands such as humics or fulvics [80], or metabolized by living organism (small or larger) and for instance being excreted in faeces [81]. Therefore, for ^{210}Po and ^{209}Po to remain in the same chemical form and in chemical equilibrium, ^{210}Po must be completely dissolved in a mineral phase, owing to the nitric acid added to the sample after collection. However, free natural ^{210}Po radicals cannot be obtained in a short elapsed time of 8 h, on the contrary, this would be possible for ^{209}Po; as a result, ^{210}Po would still be bound to organic matter or other ligands, being not easily extracted and hence recovered in lower proportion than the ^{209}Po tracer.

The results reported in Refs. [82] and [73] support this hypothesis. In Ref. [82] is obtained a consistent secular equilibrium between ^{210}Po and ^{210}Pb throughout the entire TZ. The Fe^{3+} method was applied, with the distinction that the elapsed time between acidification and the co-precipitation step was ~50 days. This period would be enough to get free natural ^{210}Po radicals, which can then be efficiently extracted along with the ^{209}Po spike by the carrier. On the other hand [73], proposed that biologically mediated Po cycling within the food web may generate dissolved Po species that are less efficiently scavenged by Fe^{3+} and require longer equilibration times with the added ^{209}Po spike, particularly when samples are processed shortly after collection.

Similar conclusions can be inferred from our groundwater samples measurements. The elapsed time between collection and co-precipitation was at least one year in these samples. In the meantime, they were stored acidified with nitric acid, which enables the acid to attack and break down the organic compounds and dissolve the salts present in the seawater [83,84], forming free ^{210}Po radicals that can be more easily extracted during the co-precipitation, together with the tracer. Additionally, it is expected that this unequal and not easily traceable extraction of ^{210}Po and ^{209}Po would be more significant in seawater than in groundwater samples, as seawater are more complex matrices due to their higher salt and organic matter content [42,85]. Accordingly [32], recently showed non-significant bias between the Fe^{3+}, Fe^{2+} and Co-APDC methods in natural water matrices. This is consistent with our results: both Fe^{3+} and Fe^{2+} methods yielded similar ^{210}Po activities in most groundwater replicates.

It is important to add that the inefficient extraction of radioisotopes from seawater using co-precipitation with Fe^{3+} is not specific to polonium. López-Lora et al. (2018) [86] reported average chemical yields of 52 ± 25 % for ^{236}U extraction using the Fe^{3+} method, which increased to 93 ± 8 % when using Fe^{2+} [35]. And for the ^{237}Np the chemical yield using Fe^{3+} is negligible, versus using co-precipitation with Fe^{2+}, where the chemical yield increases up to 87 ± 6 % [35].

The hypothesis that ^{210}Po bound to both organic matter and mineral ligands interferes with the recovery of total ^{210}Po suggests that complete oxidation of organic matter and full dissolution of the inorganic phase could lead all three methods (Co-APDC, Fe^{3+}, and Fe^{2+}) to yield comparable results, similarly to enabling the acid to release free ^{210}Po radicals.

An interesting process that reduces the interference of organic matter in the recovery of polonium and actinides when using Fe^{2+} rather than Fe^{3+} is the Fenton reaction. The Fenton reaction is an oxidation process

in which Fe^{2+} catalyzes the decomposition of H_2O_2, generating highly reactive hydroxyl radicals (• OH) [87]. Under acidic conditions, these radicals enhance the oxidation of organic matter [88]. Because this reaction does not occur with Fe^{3+}, the Fe^{2+} method may promote a higher release of ^{210}Po into the dissolved phase, resulting in recovery proportions closer to that of ^{209}Po spike by the carrier. This another reason why the use of $Fe(SO_4)_2$, Fe^{2+}, to co-precipitate ^{210}Po is more successful than the use of $Fe(OH)_3$, Fe^{3+}, since in that case the Feton reaction takes place.

In order to improve and ensure that ^{210}Po and the ^{209}Po spike are present in the same phase, a step to obtain a complete oxidation of organic matter and dissolution of mineral-associated ligands could be included. H_2O_2 and a reducing agent, e.g. ascorbic acid, could be added before the co-precipitation step, however, applying this approach onboard is operationally demanding, as it requires controlled heating for large amounts of water, several hours of treatment, and large amounts of H_2O_2 [89,90].

Thus, the results of our study, along with those reported by Refs. [27,35,86] indicate that the Fe^{2+}, Fe^{3+}, and Co-APDC methods speciate actinides and ^{210}Po differently in seawater. When ^{210}Po is extracted from the seawater matrix, the spiked ^{209}Po is not sensitive to these differences in speciation using the three different methods, as it is usually added only before the radiochemical analysis. The Fe^{2+} and Co-APDC approaches likely produce a similar speciation of natural ^{210}Po in seawater, which is extracted in the same proportion relative to ^{209}Po by both methods. The alignment within methods reported by Ref. [32] in freshwater suggests that this effect may only concern seawater matrices; in freshwater, natural ^{210}Po may be similarly speciated by the three methods, subsequently leading to consistent analytical results.

4. Conclusions

In this study, we set up a method for the determination of ^{210}Po and ^{210}Pb in seawater. This method is based on the co-precipitation of ^{210}Po and ^{209}Po with $FeSO_4$, based on Fe^{2+} formation. The method successfully measures ^{210}Po in groundwater samples and in coastal surface seawater samples and performs very well measuring on board high-resolution ^{210}Po and ^{210}Pb depth profiles in open-ocean, during two campaigns around the PAP-Site Observatory. Replicates were collected and processed using the established $Fe(OH)_3$ co-precipitation method, based on Fe^{3+}. Considerable differences in activity concentration results were observed when using the two methods, with our method providing a more accurate outcome.

The results of this study led to two main conclusions. First, the $FeSO_4$ method is suitable for the determination of ^{210}Po and ^{210}Pb in seawater, since determined activities align very well with those reported in previous studies employing the recently validated Co-APDC method. Second, the comparison of replicate samples processed with the $FeSO_4$ and $Fe(OH)_3$ methods highlights and evidence a systematic underestimation of ^{210}Po with the $Fe(OH)_3$ method. Furthermore, ^{210}Po and ^{210}Pb consistently reach the expected secular equilibrium in deep waters with Fe^{2+} co-precipitation. Whereas a systematic disequilibrium between both radioisotopes is found below the Euphotic Zone when using the Fe^{3+} method, which proves the better performance of the method based on Fe^{2+} co-precipitation.

The ^{210}Pb – ^{210}Po disequilibrium is a widely used approach to estimate downward POC fluxes [7], and any bias in the measurement of these radioisotopes activities directly affects the accuracy of the estimated sinking POC [23]. POC and ^{210}Po fluxes determined from the ^{210}Po – ^{210}Pb disequilibrium using the Fe^{2+} method showed excellent agreement with those measured by sediment traps during the APERO campaign [61], whereas the use of results obtained with the Fe^{3+} method overestimated POC fluxes in relation to those from the sediment traps.

CRediT authorship contribution statement

Á. López-Rodríguez: Validation, Investigation. **B. González-González:** Validation, Investigation. **C. García-Prieto:** Validation, Investigation. **J.L. Mas:** Validation, Supervision, Resources, Project administration, Funding acquisition. **F.A.C. Le Moigne:** Writing – review & editing, Validation, Supervision, Methodology, Investigation, Formal analysis, Conceptualization. **S.L.C. Giering:** Juan Mantero Cabrera, Validation, Investigation. **S. Hurtado-Bermúdez:** Validation, Investigation. **M. Villa-Alfageme:** Writing – original draft, Methodology, Investigation, Formal analysis, Data curation, Conceptualization.

Declaration of competing interest

The authors declare that they have no known competing financial interests or personal relationships that could have appeared to influence the work reported in this paper.

Acknowledgments AND finantial SUPPORT

We thank the captain and crew of the RSS Discovery during JC231 for their help during mobilisation. We acknowledge the use of the Sea of Thorium compilation and the Ocean Productivity database from Oregon State University, which provided essential data for this study.

This work has been funded by the SPOCK project (PID2023-149513NB-I00), supported by the Ministerio de Ciencia, Innovación y Universidades and the Fondo Europeo de Desarrollo Regional (FEDER). López-Rodríguez, A. was funded by Project Grant: DEPOCARBON (No. PCM00063), "Planes Complementarios con las Comunidades Autónomas". Plan de Recuperacion de Transformacion y Resiliencia (PRTR), Plan Complementario de I+D+I and SPOCK Project.

This Article also contributes to the APERO project funded by the National Research Agency under the grant APERO (grant no. ANR ANR-21-CE01-0027) lead by Laurent Memery, Christian Tamburini and Lionel Guidi, and by the French LEFE-Cyber programme (CNRS, INSU). The authors thank Christian Tamburini (Chief scientist), the captain and crew of N/O 'Le Pourquoi Pas' (Flotte Océanographique Française) for their help during the APERO cruise (https://doi.org/10.17600/18000066). We thank the 'Moyen Commun' SAM and Radioactivity from the Mediterranean Institute of Oceanography (MIO) as well as the 'parc national d'instrumentation océanographique' (PNIO) of the 'division technique de l'Institut national des sciences de l'Univers du CNRS (DT INSU) for their technical expertise and facilities. This work was also supported by ANR-JC ARMORIC-ANR-21 CE01-0005 granted to F.L.M.

S.L.C.G. have received funding from the European Research Council (ERC) under the European Union's Horizon 2020 research and innovation programme (grant agreement no. 950212 - ANTICS.

Appendix A. Supplementary data

Supplementary data to this article can be found online at https://doi.org/10.1016/j.talanta.2026.129812.

Data availability

All data are shared in this paper.

References

[1] R. Sanders, S.A. Henson, M. Koski, C.L. De La Rocha, S.C. Painter, A.J. Poulton, J. Riley, B. Salihoglu, A. Visser, A. Yool, R. Bellerby, A.P. Martin, The biological carbon pump in the North Atlantic, Prog. Oceanogr. 129 (2014) 200–218, https://doi.org/10.1016/j.pocean.2014.05.005.

[2] S. Henson, C. Laufkötter, S. Leung, S. Giering, H. Palevsky, E. Cavan, What the flux? Uncertain response of ocean biological carbon export in a changing world. https://doi.org/10.1002/essoar.10507873/v3, 2022.

[3] V. Puigcorbé, P. Masqué, F.A.C. Le Moigne, Global database of ratios of particulate organic carbon to thorium-234 in the ocean: improving estimates of the biological

carbon pump, Earth Syst. Sci. Data 12 (2020) 1267–1285, https://doi.org/10.5194/essd-12-1267-2020.
[4] R. Sanders, S.A. Henson, M. Koski, C.L. De La Rocha, S.C. Painter, A.J. Poulton, J. Riley, B. Salihoglu, A. Visser, A. Yool, R. Bellerby, A.P. Martin, The biological carbon pump in the North Atlantic, Prog. Oceanogr. 129 (2014) 200–218, https://doi.org/10.1016/j.pocean.2014.05.005.
[5] F.A.C. Le Moigne, Pathways of organic carbon downward transport by the Oceanic biological carbon pump, Front. Mar. Sci. 6 (2019), https://doi.org/10.3389/fmars.2019.00634.
[6] E. Ceballos-Romero, F.A.C. Le Moigne, S. Henson, C.M. Marsay, R.J. Sanders, R. García-Tenorio, M. Villa-Alfageme, Influence of bloom dynamics on Particle Export Efficiency in the North Atlantic: a comparative study of radioanalytical techniques and sediment traps, Mar. Chem. 186 (2016) 198–210, https://doi.org/10.1016/j.marchem.2016.10.001.
[7] F.A.C. Le Moigne, M. Villa-Alfageme, R.J. Sanders, C. Marsay, S. Henson, R. García-Tenorio, Export of organic carbon and biominerals derived from 234Th and 210Po at the Porcupine Abyssal Plain, Deep. Sea, Res. 1. Oceanogr. Res. Pap. 72 (2013) 88–101, https://doi.org/10.1016/j.dsr.2012.10.010.
[8] E. Verdeny, P. Masqué, J. Garcia-Orellana, C. Hanfland, J. Kirk Cochran, G. M. Stewart, POC export from ocean surface waters by means of 234Th/238U and 210Po/210Pb disequilibria: a review of the use of two radiotracer pairs, Deep. Sea, Res. 2. Top. Stud. Oceanogr. 56 (2009) 1502–1518, https://doi.org/10.1016/j.dsr2.2008.12.018.
[9] YH Li Broecker, J. cromwell, Radium-226 and radon-222: concentration in Atlantic and Pacific Ocean, Science (1967), 1979.
[10] S.E.P. Moore, E.A. Martell, Origin of 222Rn and its long-lived daughters in air over Hawaii, J. Geophys. Res. (1974).
[11] G. Lambert, B. Ardouin, G. Polian, Volcanic output of long-lived radon daughters, J. Geophys. Res. 87 (1982) 11103–11108, https://doi.org/10.1029/JC087iC13p11103.
[12] M. Villa-Alfageme, N. Briggs, E. Ceballos-Romero, F. de Soto, C. Manno, S.L. C. Giering, Seasonal variations of sinking velocities in Austral diatom blooms: lessons learned from COMICS, Deep. Sea, Res. 2. Top. Stud. Oceanogr. 213 (2024), https://doi.org/10.1016/j.dsr2.2023.105353.
[13] M. Villa-Alfageme, F. De Soto, F.A.C. Le Moigne, S.L.C. Giering, R. Sanders, R. García-Tenorio, Observations and modeling of slow-sinking particles in the twilight zone, Glob. Biogeochem. Cycles 28 (2014) 1327–1342, https://doi.org/10.1002/2014GB004981.
[14] M. Villa-Alfageme, J.L. Mas, S. Hurtado-Bermudez, P. Masqué, Rapid determination of 210Pb and 210Po in water and application to marine samples, Talanta 160 (2016) 28–35, https://doi.org/10.1016/j.talanta.2016.06.051.
[15] G. Stewart, J. Kirk Cochran, J. Xue, C. Lee, S.G. Wakeham, R.A. Armstrong, P. Masqué, J. Carlos Miquel, Exploring the connection between 210Po and organic matter in the northwestern Mediterranean, Deep. Sea, Res. 1. Oceanogr. Res. Pap. 54 (2007) 415–427, https://doi.org/10.1016/j.dsr.2006.12.006.
[16] K.M. Matthews, C.K. Kim, P. Martin, Determination of 210Po in environmental materials: a review of analytical methodology, Appl. Radiat. Isot. 65 (2007) 267–279, https://doi.org/10.1016/j.apradiso.2006.09.005.
[17] M. Roca-Martí, V. Puigcorbé, 31:23 Annual Review of Marine Science Downloaded from, 2024, https://doi.org/10.1146/annurev-marine-041923. www.annualreviews.org.Guest(guest. IP: 193.147.173.140 On: Fri.
[18] A.P. Fleer, M.P. Bacon, Determination of 210Pb and 210Po in Seawater and Marine Particulate Matter, 1984.
[19] M. Roca-Martí, V. Puigcorbé, 31:23 Annual Review of Marine Science Downloaded from, 2024, https://doi.org/10.1146/annurev-marine-041923. www.annualreviews.org.Guest(guest. IP: 193.147.173.140 On: Fri.
[20] P. Thakur, A.L. Ward, 210Po in the environment: insight into the naturally occurring polonium isotope, J. Radioanal. Nucl. Chem. 323 (2020) 27–49, https://doi.org/10.1007/s10967-019-06939-2.
[21] J.K. Cochran, M.P. Bacon, S. Krishnaswami, K.K. Turekian, 21°po and 21°pb Distributions in the Central and Eastern Indian Ocean, 1983.
[22] Y. Chung, H. Craig, 21°pb in the Pacific: the GEOSECS Measurements of Particulate and Dissolved Concentrations, Elsevier Science Publishers B.V, 1983.
[23] T. Church, S. Rigaud, M. Baskaran, A. Kumar, J. Friedrich, P. Masque, V. Puigcorbé, G. Kim, O. Radakovitch, G. Hong, H. Choi, G. Stewart, Intercalibration studies of 210Po and 210Pb in dissolved and particulate seawater samples, Limnol Oceanogr. Methods 10 (2012) 776–789, https://doi.org/10.4319/lom.2012.10.776.
[24] G. Kim, Large De¢Ciency of Polonium in the Oligotrophic Ocean's Interior, 2001. www.elsevier.com/locate/epsl.
[25] G. Kim, N. Hussain, T.M. Church, H.-S. Yang, A Practical and Accurate Method for the Determination of 234 Th Simultaneously with 210 Po and 210 Pb in Seawater, 1999.
[26] S. Rigaud, G. Stewart, M. Baskaran, D. Marsan, T. Church, 210Po and 210Pb distribution, dissolved-particulate exchange rates, and particulate export along the North Atlantic US GEOTRACES GA03 section, Deep. Sea, Res. 2. Top. Stud. Oceanogr. 116 (2015) 60–78, https://doi.org/10.1016/j.dsr2.2014.11.003.
[27] M. Roca-Martí, V. Puigcorbé, M. Castrillejo, N. Casacuberta, J. Garcia-Orellana, J. K. Cochran, P. Masqué, Quantifying 210Po/210Pb disequilibrium in seawater: a comparison of two precipitation methods with differing results, Front. Mar. Sci. 8 (2021), https://doi.org/10.3389/fmars.2021.684484.
[28] Harold Carrasco, J.K. Cochran, Beat Gasser, Inés Sanz-Alvarez, M. Roca-Martí, C. Heilbrun, N.S. Fisher, J. Friedrich, P. Masqué, Comparing Methods for Measuring 210Po in Seawater: Fe(Oh)3 can Extract less 210Po than Co-APDC and Thus Overestimate POC Export Fluxes, 2025. Preprint.
[29] C. Katzlberger, G. Wallner, K. Irlweck, Determination of 210 Pb, 210 Bi and 210 Po in Natural Drinking Water, 2001.
[30] N. Vajda, J. Larosaa, R. Zeisler, P. Danesi', G. Kis-Benedek', A Novel Technique for the Simultaneous Determination of 210Pb and 210Po Using a Crown Ether, 1997.
[31] J.T. Waples, Measuring bismuth-210, its parent, and daughter in aquatic systems, Limnol Oceanogr. Methods 18 (2020) 148–162, https://doi.org/10.1002/lom3.10352.
[32] J.T. Waples, G.J. Hunter, R.A. Smith, Measuring 210Po in natural waters: a comparison of three methods with similar results, J. Environ. Radioact. 288 (2025), https://doi.org/10.1016/j.jenvrad.2025.107732.
[33] E. Chamizo, M. López-Lora, M. Bressac, I. Levy, M.K. Pham, Excess of 236U in the northwest Mediterranean Sea, Sci. Total Environ. 565 (2016) 767–776, https://doi.org/10.1016/j.scitotenv.2016.04.142.
[34] M. López-Lora, E. Chamizo, M. Rožmarić, D.C. Louw, Presence of 236U and 237Np in a marine ecosystem: the northern Benguela Upwelling System, a case study, Sci. Total Environ. 708 (2020), https://doi.org/10.1016/j.scitotenv.2019.135222.
[35] M. López-Lora, I. Levy, E. Chamizo, Simple and fast method for the analysis of 236U, 237Np, 239Pu and 240Pu from seawater samples by Accelerator Mass Spectrometry, Talanta 200 (2019) 22–30, https://doi.org/10.1016/j.talanta.2019.03.036.
[36] IAEA Analytical Quality, Nuclear Applications No. IAEA/AQ/12, Determination of Po-210 in water, in: https://www.iaea.org/publications/8200/a-procedure-for-determination-of-po-210-in-water-samples-by-alpha-spectrometry, 2009.
[37] S.E. Hartman, B.J. Bett, J.M. Durden, S.A. Henson, M. Iversen, R.M. Jeffreys, T. Horton, R. Lampitt, A.R. Gates, Enduring science: three decades of observing the Northeast Atlantic from the Porcupine Abyssal Plain Sustained Observatory (PAP-SO), Prog. Oceanogr. 191 (2021), https://doi.org/10.1016/j.pocean.2020.102508.
[38] M. Gesson, F.A. C Le Moigne, M. Villa Alfageme, Particle Flux Attenuation in Northeast Atlantic During APERO, 2025.
[39] P. Thakur, A.L. Ward, 210Po in the environment: insight into the naturally occurring polonium isotope, J. Radioanal. Nucl. Chem. 323 (2020) 27–49, https://doi.org/10.1007/s10967-019-06939-2.
[40] S. Rigaud, V. Puigcorbé, P. Cámara-Mor, N. Casacuberta, M. Roca-Martí, J. Garcia-Orellana, C.R. Benitez-Nelson, P. Masqué, T. Church, A methods assessment and recommendations for improving calculations and reducing uncertainties in the determination of 210Po and 210Pb activities in seawater, Limnol Oceanogr. Methods 11 (2013) 561–571, https://doi.org/10.4319/lom.2013.11.561.
[41] W. Lin, H. Ma, L. Chen, Z. Zeng, J. He, S. Zeng, Decay/ingrowth uncertainty correction of 210Po/210Pb in seawater, J. Environ. Radioact. 137 (2014) 22–30, https://doi.org/10.1016/j.jenvrad.2014.06.005.
[42] M. Villa-Alfageme, J.L. Mas, S. Hurtado-Bermudez, P. Masqué, Rapid determination of 210Pb and 210Po in water and application to marine samples, Talanta 160 (2016) 28–35, https://doi.org/10.1016/j.talanta.2016.06.051.
[43] D.B. Sharma, V.N. Jha, S. Singh, N.K. Sethy, S.K. Sahoo, S.K. Jha, M.S. Kulkarni, Distribution of 210Pb and 210Po in ground water around uranium mineralized area of Jaduguda, Jharkhand, India, J. Radioanal. Nucl. Chem. 327 (2021) 217–227, https://doi.org/10.1007/s10967-020-07495-w.
[44] S.M. Pérez-Moreno, J.L. Guerrero, F. Mosqueda, M.J. Gázquez, J.P. Bolívar, Hydrochemical behaviour of long-lived natural radionuclides in Spanish groundwaters, Catena 191 (2020), https://doi.org/10.1016/j.catena.2020.104558.
[45] K.M. Dias da Cunha, H. Henderson, B.M. Thomson, A.A. Hecht, Ground water contamination with 238U, 234U, 235U, 226Ra and 210Pb from past uranium mining: cove wash, Arizona, Environ. Geochem. Health 36 (2014) 477–487, https://doi.org/10.1007/s10653-013-9575-2.
[46] Y. Chung, T. Wu, Large 210Po deficiency in the northern South China Sea, Cont. Shelf Res. 25 (2005) 1209–1224, https://doi.org/10.1016/j.csr.2004.12.016.
[47] C. Gascó, M.P. Antón, R. Delfanti, A.M. González, J. Meral, C. Papucci, Variation of the Activity Concentrations and Fluxes of Natural (210 Po, 210 Pb) and Anthropogenic (239,240 Pu, 137 Cs) Radionuclides in the Strait of Gibraltar (Spain), 2002. www.elsevier.com/locate/jenvrad.
[48] C. Gasco, M.P. Anton, IAEA-SM-354/260P XA9952092 Plutonium and Polonium Concentrations in the Different Water Masses Crossing the Strait of Gibraltar, 1999.
[49] P. Masqué, J.A. Sanchez-Cabeza, J.M. Bruach, E. Palacios, M. Canals, Balance and Residence Times of 210 Pb and 210 Po in Surface Waters of the Northwestern Mediterranean Sea, 2002.
[50] M.A. Meli, D. Desideri, A. Penna, F. Ricci, C. Roselli, 210 Po and 210 Pb concentration in environmental samples of the adriatic Sea, Int. J. Environ. Res. 7 (2013) 51–60.
[51] M.A. Meli, D. Desideri, C. Roselli, L. Feduzi, Analytical methods to determine 210Po and 210Pb in marine samples, Microchem. J. 99 (2011) 273–277, https://doi.org/10.1016/j.microc.2011.05.013.
[52] C. Gascó, M.P. Antón, R. Delfanti, A.M. González, J. Meral, C. Papucci, Variation of the Activity Concentrations and Fluxes of Natural (210 Po, 210 Pb) and Anthropogenic (239,240 Pu, 137 Cs) Radionuclides in the Strait of Gibraltar (Spain), 2002. www.elsevier.com/locate/jenvrad.
[53] E.J. Horowitz, J.K. Cochran, M.P. Bacon, D.J. Hirschberg, 210Po and 210Pb distributions during a phytoplankton bloom in the North Atlantic: implications for POC export, Deep. Sea, Res. 1. Oceanogr. Res. Pap. 164 (2020), https://doi.org/10.1016/j.dsr.2020.103339.
[54] Y. Tang, G. Stewart, The 210Po/210Pb method to calculate particle export: lessons learned from the results of three GEOTRACES transects, Mar. Chem. 217 (2019), https://doi.org/10.1016/j.marchem.2019.103692.
[55] J.F. Marra, V.P. Lance, R.D. Vaillancourt, B.R. Hargreaves, Resolving the ocean's euphotic zone, Deep. Sea, Res. 1. Oceanogr. Res. Pap. 83 (2014) 45–50, https://doi.org/10.1016/j.dsr.2013.09.005.

[56] K.O. Buesseler, P.W. Boyd, E.E. Black, D.A. Siegel, D.A.S. Designed, E.E. B. Performed, Metrics that matter for assessing the ocean biological carbon pump. https://doi.org/10.1073/pnas.1918114117/-/DCSupplemental, 2020.
[57] J. Cherrier, W.C. Burnett, P.A. LaRock, Uptake of polonium and sulfur by bacteria, Geomicrobiol. J. 13 (1995) 103–115, https://doi.org/10.1080/01490459509378009.
[58] P. Larock, J.-H. Hyun, L.S. Boutelle, W.C. Burnett, C.D. Hull, Bacterial Mobilization of Polonium, 1996.
[59] G.M. Stewart, N.S. Fisher, Bioaccumulation of polonium-210 in marine copepods, Limnol. Oceanogr. 48 (2003) 2011–2019, https://doi.org/10.4319/lo.2003.48.5.2011.
[60] R. Idoeta, M. Herranz, F. Legarda, The disequilibrium between 210Po and 210Pb in raw and drinking waters, Appl. Radiat. Isot. 69 (2011) 196–200, https://doi.org/10.1016/j.apradiso.2010.07.021.
[61] Á. López Rodríguez, B. González González, S. Hurtado Bermúdez, F. Le Moigne, M. Gesson, M. Villa Alfageme, Analysis of Export and Transfer Efficiency Around the PAP-Site Observatory: an Update from the APERO Project, 2025, https://doi.org/10.5194/egusphere-egu25-13345.
[62] D.M. Bonotto, L. Caprioglio, T.O. Bueno, J.R. Lazarindo, Dissolved 210Po and 210Pb in Guarani aquifer groundwater, Brazil, Radiat. Meas. 44 (2009) 311–324, https://doi.org/10.1016/j.radmeas.2009.03.022.
[63] S.R. Ruberu, Y.-G. Liu, S.K. Perera, Ocurrence and distribution of 210Pb and 210Po in selected California groundwater wells, Health Phys. (2007), https://doi.org/10.1097/01.HP.0000254883.26386.9b.
[64] P. Vesterbacka, T.K. Ikäheimonen, Optimization of 210Pb determination via spontaneous deposition of 210Po on a silver disk, Anal. Chim. Acta 545 (2005) 252–261, https://doi.org/10.1016/j.aca.2005.04.074.
[65] H. Kawakami, M.C. Honda, S. Watanabe, T. Sino, Time-series observations of 210Po and 210Pb radioactivity in the western North Pacific, J. Radioanal. Nucl. Chem. 301 (2014) 461–468, https://doi.org/10.1007/s10967-014-3141-y.
[66] Q. Zhong, V. Puigcorbé, C. Sanders, J. Du, Analysis of 210Po, 210Bi, and 210Pb in atmospheric and oceanic samples by simultaneously auto-plating 210Po and 210Bi onto a nickel disc, J. Environ. Radioact. (2020) 220–221, https://doi.org/10.1016/j.jenvrad.2020.106301.
[67] G. Stewart, J. Kirk Cochran, J. Xue, C. Lee, S.G. Wakeham, R.A. Armstrong, P. Masqué, J. Carlos Miquel, Exploring the connection between 210Po and organic matter in the northwestern Mediterranean, Deep. Sea, Res. 1. Oceanogr. Res. Pap. 54 (2007) 415–427, https://doi.org/10.1016/j.dsr.2006.12.006.
[68] W. Yang, L. Guo, C.Y. Chuang, D. Schumann, M. Ayranov, P.H. Santschi, Adsorption characteristics of 210Pb, 210Po and 7Be onto micro-particle surfaces and the effects of macromolecular organic compounds, Geochim. Cosmochim. Acta 107 (2013) 47–64, https://doi.org/10.1016/j.gca.2012.12.039.
[69] F. De Soto, E. Ceballos-Romero, M. Villa-Alfageme, A microscopic simulation of particle flux in ocean waters: application to radioactive pair disequilibrium, Geochim. Cosmochim. Acta 239 (2018) 136–158, https://doi.org/10.1016/j.gca.2018.07.031.
[70] C.L. Wei, M.C. Yi, S.Y. Lin, L.S. Wen, W.H. Lee, Seasonal distributions and fluxes of 210Pb and 210Po in the northern South China Sea, Biogeosciences 11 (2014) 6813–6826, https://doi.org/10.5194/bg-11-6813-2014.
[71] Bath, et al., 234Th/238U ratios in the Ocean. https://doi.org/10.1016/S0012-821X(68)80083-4, 1969.
[72] L. Zhou, R. Wang, H. Ren, P. Wang, Y. Cao, Detection of Polonium-210 in environmental, biological and food samples: a review, Molecules 28 (2023), https://doi.org/10.3390/molecules28176268.
[73] H. Carrasco, J.K. Cochran, B. Gasser, I. Sanz-Alvarez, M. Roca-Martí, C. Heilbrun, N.S. Fisher, J. Friedrich, P. Masqué, Comparing methods for measuring 210Po in seawater: Fe(OH)3 can extract less 210Po than Co-APDC and thus overestimate POC export fluxes, Mar. Chem. 275 (2026), https://doi.org/10.1016/j.marchem.2026.104618.
[74] M. Roca-Martí, V. Puigcorbé, M.M. Rutgers van der Loeff, C. Katlein, M. Fernández-Méndez, I. Peeken, P. Masqué, Carbon export fluxes and export efficiency in the central Arctic during the record sea-ice minimum in 2012: a joint 234Th/238U and 210Po/210Pb study, J. Geophys. Res., Oceans 121 (2016) 5030–5049, https://doi.org/10.1002/2016JC011816.
[75] Kimberly A. Roberts, J.K. Cochran, Christina Barnes, 210Pb and 239,240Pu in the Northeast Water Polynya, Greenland: Particle Dynamics and Sediment Mixing Rates, 1996.
[76] Y. Tang, M. Castrillejo, M. Roca-Martí, P. Masqué, N. Lemaitre, G. Stewart, Distributions of total and size-fractionated particulate 210Po and 210Pb activities along the North Atlantic GEOTRACES GA01 transect: GEOVIDE cruise, Biogeosciences 15 (2018) 5437–5453, https://doi.org/10.5194/bg-15-5437-2018.
[77] R.M. Moore, J.N. Smith, Disequilibria Between 226 Ra, 210 Pb and 210 Po in the Arctic Ocean and the Implications for Chemical Modification of the Pacific Water Inflow, 1986.
[78] J.N. Smith, S.B. Moran, R.W. Macdonald, Shelf-basin interactions in the Arctic Ocean based on 210Pb and Ra isotope tracer distributions, Deep. Sea, Res. 1. Oceanogr. Res. Pap. 50 (2003) 397–416, https://doi.org/10.1016/S0967-0637(02)00166-8.
[79] M. Nowicki, T. DeVries, D.A. Siegel, Quantifying the carbon export and sequestration pathways of the ocean's biological carbon pump, Glob. Biogeochem. Cycles 36 (2022), https://doi.org/10.1029/2021GB007083.
[80] M. Antony Wildgust, Behaviour of 210Po in the Marine Environment, 1998.
[81] S. Uddin, S.W. Fowler, M. Behbehani, M. Metian, 210Po bioaccumulation and trophic transfer in marine food chains in the northern Arabian Gulf, J. Environ. Radioact. 174 (2017) 23–29, https://doi.org/10.1016/j.jenvrad.2016.08.021.
[82] Q. Ma, Y. Qiu, R. Zhang, E. Lv, Y. Huang, M. Chen, 210Po/210Pb Disequilibria in the Eastern tropical north Pacific, Front. Mar. Sci. 8 (2021), https://doi.org/10.3389/fmars.2021.716688.
[83] D.A. Hansell, Recalcitrant dissolved organic carbon fractions, Ann. Rev. Mar. Sci 5 (2013) 421–445, https://doi.org/10.1146/annurev-marine-120710-100757.
[84] Xiaoxuan Zheng, Ruanhong Cai, Hongwei Yao, Xiaocun Zhuo, Chen He, Qiang Zheng, Quan Shi, Nianzhi Jiao, Experimental Insight into the enigmatic persistence refractory dissolved organic matter, Environmental Science & Techonology (2022).
[85] M. Bayani Cardenas Conolly, Greta A. Burkart, Robert G.M. Spencer, James W. McClelland, Groundwater as a major source of dissolved organic matter to Artic coastal waters, Nat. Commun. (2020).
[86] M. López-Lora, E. Chamizo, M. Villa-Alfageme, S. Hurtado-Bermúdez, N. Casacuberta, M. García-León, Isolation of 236U and 239,240Pu from seawater samples and its determination by Accelerator Mass Spectrometry, Talanta 178 (2018) 202–210, https://doi.org/10.1016/j.talanta.2017.09.026.
[87] W.H. Koppenol, The Centennial of the Fenton Reaction, 1993.
[88] C. Zheng, L. Zhao, X. Zhou, Z. Fu, A. Li, Treatment technologies for organic wastewater, in: Water Treatment, InTech, 2013, https://doi.org/10.5772/52665.
[89] D.W. Nelson, L.E. Sommers, Total carbon, organic carbon, and organic matter. https://doi.org/10.2136/sssabookser5.3.c34, 1996.
[90] M. Sinojmeri, C. Landstetter, C. Katzlberger, A. Achatz, Rapid Method for Determination of Po Isotopes in Biological Matter, 2012.